JOC Article

Synthesis and Characterization of Water-Soluble Phenylene−Vinylene-Based Singlet Oxygen Sensitizers for Two-Photon Excitation

Christian B. Nielsen,[†,‡] Mette Johnsen,[‡] Jacob Arnbjerg,[‡] Michael Pittelkow,[§] Sean P. McIlroy,[‡] Peter R. Ogilby,*[,‡] and Mikkel Jørgensen*[,†]

Polymer Department, Risø National Laboratory, Frederiksborgvej 399, DK-4000 Roskilde, Denmark, Department of Chemistry, University of Aarhus, Langelandsgade 140, DK-8000, Århus C, Denmark, and Department of Chemistry, University of Copenhagen, Universitetsparken 5, DK-2100, Copenhagen Ø, Denmark

progilby@chem.au.dk

Received March 14, 2005

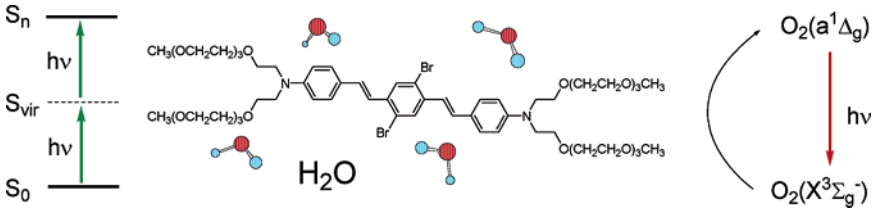

The synthesis and characterization of water-soluble singlet oxygen sensitizers with a phenylene−vinylene motif is presented. The principal motivation for this study was to better understand specific features of a water-soluble molecule that influence the photosensitized production of singlet oxygen upon nonlinear, two-photon excitation of that molecule. To achieve water solubility, sensitizers were synthesized with ionic as well as nonionic substituents. In the ionic approach, salts of *N*-methylated pyridine, benzothiazole, and 1-methyl-piperazine moieties were used, as were aryl-substituted sulfonic acid moieties. In the nonionic approach, aryl-substituted triethylene glycol moieties were used. Selected photophysical properties of the compounds synthesized were determined, including singlet oxygen quantum yields. Of the molecules examined, the most efficient singlet oxygen sensitizers had triethylene glycol units as the functional group that imparted water solubility. Molecules containing the ionic moieties did not make singlet oxygen in appreciable yield nor did they efficiently fluoresce. Rather, for these latter molecules, rapid charge-transfer-mediated nonradiative processes appear to dominate excited state deactivation.

Introduction

Nonlinear, two-photon excitation of organic molecules has received a great deal of recent attention as an alternative to linear, one-photon excitation due to promising spatially resolved applications in 3D microstructuring, imaging, and photodynamic therapy.[1−9] In the two-photon absorption (TPA) process, the production of a given electronic excited state is achieved via the simultaneous absorption of two photons of comparatively low energy. As such, the two-photon experiments are performed by irradiating the sample at wavelengths where dominant one-photon transitions are generally absent. This means that one can achieve better depth penetration in a sample. Moreover, because the probability of absorbing two photons increases quadratically

[†] Risø National Laboratory.
[‡] University of Aarhus.
[§] University of Copenhagen.

(1) Albota, M.; Beljonne, D.; Brédas, J.-L.; Ehrlich, J. E.; Fu, J.-Y.; Heikal, A. A.; Hess, S. E.; Kogej, T.; Levin, M. D.; Marder, S. R.; McCord-Maughon, D.; Perry, J. W.; Röckel, H.; Rumi, M.; Subramaniam, G.; Webb, W. W.; Wu, X.-L.; Xu, C. *Science* **1998**, *281*, 1653−1656.
(2) Denk, W.; Strickler, J. H.; Webb, W. W. *Science* **1990**, *248*, 73−76.
(3) Porres, L.; Mongin, O.; Katan, C.; Charlot, M.; Pons, T.; Mertz, J.; Blanchard-Desce, M. *Org. Lett.* **2004**, *6*, 47−50.
(4) Iwase, Y.; Kamada, K.; Ohta, K.; Kondo, K. *J. Mater. Chem.* **2003**, *13*, 1575−1581.
(5) Pyun, O. K.; Yang, W.; Jeong, M.-Y.; Lee, S. H.; Kang, K. M.; Jeon, S.-J.; Cho, B. R. *Tetrahedron Lett.* **2003**, *44*, 5179−5182.
(6) Strehmel, B.; Sarker, A. M.; Detert, H. *ChemPhysChem* **2003**, *4*, 249−259.
(7) Kawata, S.; Sun, H.-B.; Tanaka, T.; Takada, K. *Nature* **2001**, *412*, 697−698.
(8) Reinhardt, B. A.; Brott, L. L.; Clarson, S. J.; Dillard, A. G.; Bhatt, J. C.; Kannan, R.; Yuan, L.; He, G. S.; Prasad, P. N. *Chem. Mater.* **1998**, *10*, 1863−1874.
(9) King, B. A.; Oh, D. H. *Photochem. Photobiol.* **2004**, *80*, 1−6.

10.1021/jo050507y CCC: $30.25
Published on Web 08/11/2005

with the photon flux, excited state production can be limited to a small volume defined by a focused laser where a sufficiently high fluence is obtained.

It is acknowledged that singlet molecular oxygen ($a^1\Delta_g$) is an important reactive intermediate in many photoinduced oxidations,[10,11] including those involved in photodynamic therapy.[12] We have embarked on an extensive program to develop methods by which singlet oxygen can be generated in, and optically detected from, small spatially resolved domains in heterogeneous samples.[13−18] To this end, the two-photon photosensitized production of singlet oxygen and the associated development of the appropriate sensitizer molecules are important issues.[19−22]

A substantial amount of work has been done in the recent past on the development of molecules that have comparatively large two-photon absorption probabilities (i.e., the so-called TPA cross section).[1,8] Most of these molecules, however, have been designed for fluorescence experiments and are not suitable for use as singlet oxygen sensitizers. Molecules used as singlet oxygen sensitizers generally undergo efficient intersystem crossing to produce the lowest triplet state, which in turn must efficiently transfer its excitation energy to ground state oxygen to yield singlet oxygen. As such, one design strategy to make singlet oxygen sensitizers is to introduce functional groups into the chromophore that facilitate intersystem crossing (e.g., carbonyl groups or heavy atoms such as bromine). Other features of a good singlet oxygen sensitizer may include stability upon prolonged irradiation and the lack of appreciable luminescence in the near-infrared that could interfere with the optical detection of the weak singlet oxygen phosphorescence signal at 1270 nm.

A host of oligo phenylene vinylenes (OPVs) with comparatively large TPA cross sections have recently been prepared.[1,23] It has been ascertained that, with these compounds, the two-photon transition probability increases with an increase in the degree of intramolecular charge transfer (CT) upon excitation (i.e., large transition moments are desirable).[1,20,23−25] As such, the judicious introduction of electron donor and acceptor groups in the molecule can significantly enhance the two-photon absorption probability. Longer conjugation lengths that result in larger charge separation in the molecule are also beneficial for obtaining large TPA cross sections.[1,23,26]

We have shown that some OPV molecules can also generate singlet oxygen.[19−22] It has also been shown, however, that the extent of CT character, both within a given molecule and in a given molecule−oxygen complex, can have a large effect on the efficiency with which singlet oxygen is generated.[27−30] In general, CT character in a sensitizer−oxygen complex facilitates nonradiative deactivation of the excited state at the expense of energy transfer from the sensitizer to produce singlet oxygen. As such, and in the present context of developing two-photon sensitizers, CT character in a molecule is not desired (in this argument, we assume that the extent of intermolecular CT character in the sensitizer−oxygen complex will be larger for a sensitizer with a proclivity for intramolecular charge transfer). The extent to which this CT effect is manifested also depends significantly on the polarity of the solvent in which the system is dissolved.[22,28,29,31] Generally, CT character is enhanced in more polar solvents such as water or acetonitrile, which, in turn, results in comparatively low singlet oxygen yields. It is with these points in mind that we have investigated the extent to which singlet oxygen can be produced in a two-photon photosensitized process in aqueous systems.

We have demonstrated that the two-photon photosensitized production of singlet oxygen in water can be a complicated problem.[22] Specifically, functional groups on the sensitizer that impart water solubility and that give rise to larger TPA cross sections are, in many cases, not conducive to the production of singlet oxygen in high yield. In part, this issue involves the competing influence of charge transfer, not just in the sensitizer itself but in the sensitizer−oxygen complex as well. As already mentioned, molecular features that increase CT character in the chromophore facilitate two-photon absorption, whereas these same features contribute to a low singlet oxygen yield.

In this present article, we continue our study of issues pertinent to the development of water-soluble, two-photon singlet oxygen sensitizers.[22] In particular, we now focus on the synthesis and characterization of some phenylene−vinylene-based molecules.

(10) Foote, C. S. *Acc. Chem. Res.* **1968**, *1*, 104−110.
(11) *Singlet Oxygen*; Frimer, A. A., Ed.; CRC Press: Boca Raton, FL, 1985; Vols. I−IV.
(12) Dougherty, T. J.; Gomer, C. J.; Henderson, B. W.; Jori, G.; Kessel, D.; Korbelik, M.; Moan, J.; Peng, Q. *J. Natl. Cancer Inst.* **1998**, *90*, 889−905.
(13) Skovsen, E.; Snyder, J. W.; Lambert, J. D. C.; Ogilby, P. R. *J. Phys. Chem. B* **2005**, *109*, 8570−8573.
(14) Snyder, J. W.; Gao, Z.; Ogilby, P. R. *Rev. Sci. Instrum.* **2005**, *76*, 013701.
(15) Snyder, J. W.; Zebger, I.; Gao, Z.; Poulsen, L.; Frederiksen, P. K.; Skovsen, E.; McIlroy, S. P.; Klinger, M.; Andersen, L. K.; Ogilby, P. R. *Acc. Chem. Res.* **2004**, *37*, 894−901.
(16) Zebger, I.; Snyder, J. W.; Andersen, L. K.; Poulsen, L.; Gao, Z.; Lambert, J. D. C.; Kristiansen, U.; Ogilby, P. R. *Photochem. Photobiol.* **2004**, *79*, 319−322.
(17) Zebger, I.; Poulsen, L.; Gao, Z.; Andersen, L. K.; Ogilby, P. R. *Langmuir* **2003**, *19*, 8927−8933.
(18) Andersen, L. K.; Gao, Z.; Ogilby, P. R.; Poulsen, L.; Zebger, I. *J. Phys. Chem. A* **2002**, *106*, 8488−8490.
(19) Frederiksen, P. K.; Jørgensen, M.; Ogilby, P. R. *J. Am. Chem. Soc.* **2001**, *123*, 1215−1221.
(20) Poulsen, T. D.; Frederiksen, P. K.; Jørgensen, M.; Mikkelsen, K. V.; Ogilby, P. R. *J. Phys. Chem. A* **2001**, *105*, 11488−11495.
(21) McIlroy, S. P.; Cló, E.; Nikolajsen, L.; Frederiksen, P. K.; Nielsen, C. B.; Mikkelsen, K. V.; Gothelf, K. V.; Ogilby, P. R. *J. Org. Chem.* **2005**, *70*, 1134−1146.
(22) Frederiksen, P. K.; McIlroy, S. P.; Nielsen, C. B.; Nikolajsen, L.; Skovsen, E.; Jørgensen, M.; Mikkelsen, K. V.; Ogilby, P. R. *J. Am. Chem. Soc.* **2005**, *127*, 255−269.
(23) Pond, S. J. K.; Rumi, M.; Levin, M. D.; Parker, T. C.; Beljonne, D.; Day, M. W.; Brédas, J.-L.; Marder, S. R.; Perry, J. W. *J. Phys. Chem. A* **2002**, *106*, 11470−11480.
(24) Wang, C.-K.; Macak, P.; Luo, Y.; Ågren, H. *J. Chem. Phys.* **2001**, *114*, 9813−9820.
(25) Norman, P.; Luo, Y.; Ågren, H. *J. Chem. Phys.* **1999**, *111*, 7758−7765.
(26) Drobizhev, M.; Karotki, A.; Rebane, A.; Spangler, C. W. *Opt. Lett.* **2001**, *26*, 1081−1083.
(27) Schweitzer, C.; Schmidt, R. *Chem. Rev.* **2003**, *103*, 1685−1757.
(28) Kristiansen, M.; Scurlock, R. D.; Iu, K.-K.; Ogilby, P. R. *J. Phys. Chem.* **1991**, *95*, 5190−5197.
(29) McGarvey, D. J.; Szekeres, P. G.; Wilkinson, F. *Chem. Phys. Lett.* **1992**, *199*, 314−319.
(30) Schmidt, R.; Shafii, F.; Schweitzer, C.; Abdel-Shafi, A. A.; Wilkinson, F. *J. Phys. Chem. A* **2001**, *105*, 1811−1817.
(31) Abdel-Shafi, A. A.; Wilkinson, F. *Phys. Chem. Chem. Phys.* **2002**, *4*, 248−254.

SCHEME 1. Synthesis of the MTEG-Substituted OPV Sensitizers

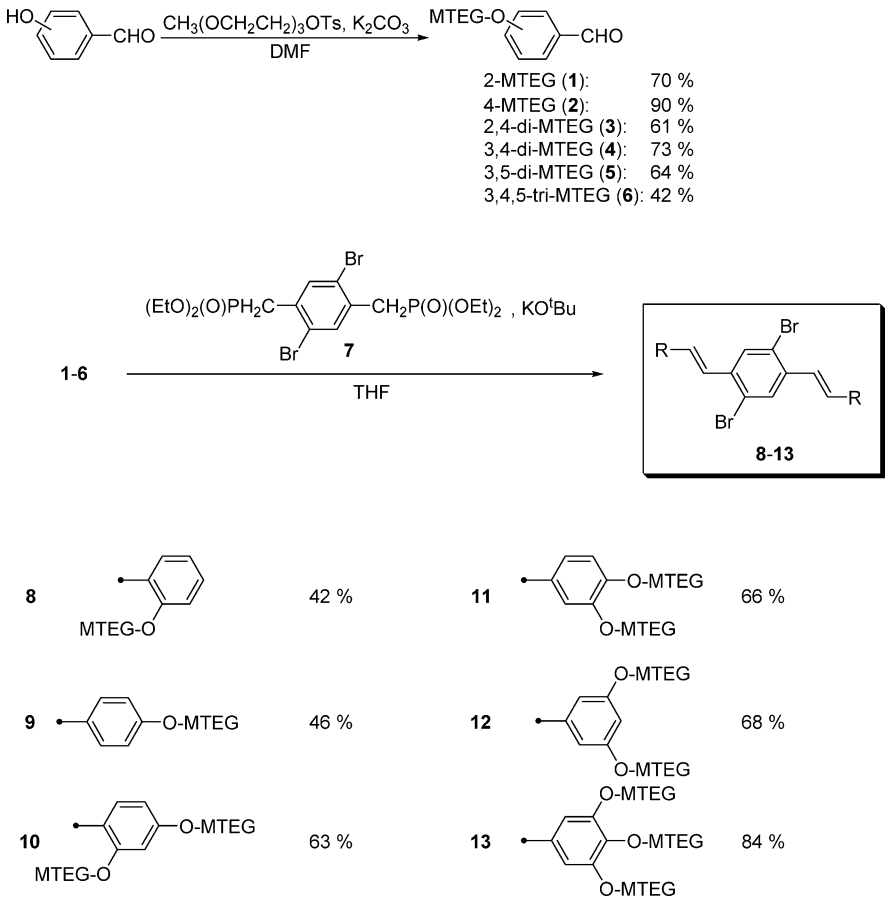

CHART 1. General Structure of the Sensitizers Examined in the Present Work[a]

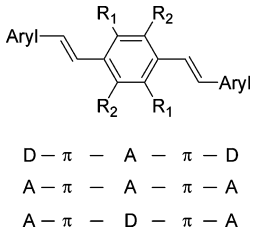

D − π − A − π − D
A − π − A − π − A
A − π − D − π − A

[a] The letters A and D refer to electron acceptors and donors, respectively, and illustrate methods by which substituents can be used to influence the electronic character of the chromophore.

SCHEME 2. Preparation of 3,4,5-Triacetoxy-benzaldehyde

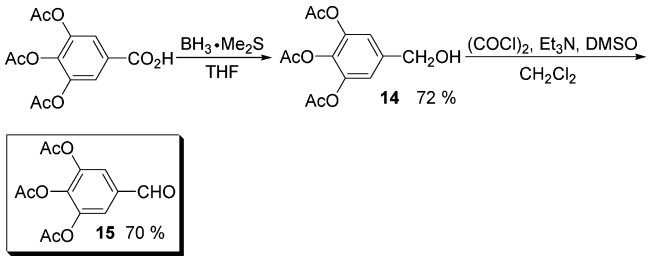

Results and Discussion

All the molecules examined in the present work were prepared following design principles that have evolved in the development of OPVs with large TPA cross sections (Chart 1).[1,6,23,32−34]

The molecules are centrosymmetric and are built around a core aromatic ring with vinyl substituents in the 1- and 4-positions. In this study, the functional groups used to impart solubility in water are attached to the chromophoric π system. As such, their electron-donating or -accepting properties also influence the extent to which CT character plays a role in the photophysics of the molecule. The substituents employed include nonionic monomethyl-ether triethylene glycol moieties (MTEGs) and ionic *N*-methylated species. Bromine atoms were also incorporated into most of the molecules studied to facilitate intersystem crossing to the triplet state.

Synthesis. For the nonionic sensitizers, MTEG moieties were used to impart water solubility. The synthesis of these molecules is outlined in Scheme 1. Briefly, Horner−Wadsworth−Emmons (HWE) reactions were used to couple the core aromatic ring of the OPV to the terminal, MTEG-substituted aryl moieties. The MTEG-substituted benzaldehydes were prepared from the hydroxy-substituted benzaldehydes in an S_N2 reaction with the tosylated glycol.

(32) Beljonne, D.; Wenseleers, W.; Zojer, E.; Shuai, Z.; Vogel, H.; Pond, S. J. K.; Perry, J. W.; Marder, S. R.; Brédas, J.-L. *Adv. Funct. Mater.* **2002**, *12*, 631−641.
(33) Rumi, M.; Ehrlich, J. E.; Heikal, A. A.; Perry, J. W.; Barlow, S.; Hu, Z.; McCord-Maughon, D.; Parker, T. C.; Röckel, H.; Thayumanavan, S.; Marder, S. R.; Beljonne, D.; Brédas, J.-L. *J. Am. Chem. Soc.* **2000**, *122*, 9500−9510.
(34) Zojer, E.; Beljonne, D.; Kogej, T.; Vogel, H.; Marder, S. R.; Perry, J. W.; Brédas, J. L. *J. Chem. Phys.* **2002**, *116*, 3646−3658.

SCHEME 3. Synthesis of a MTEG-Substituted OPV, Where the MTEG Groups Are Attached to an Amino-ethanol

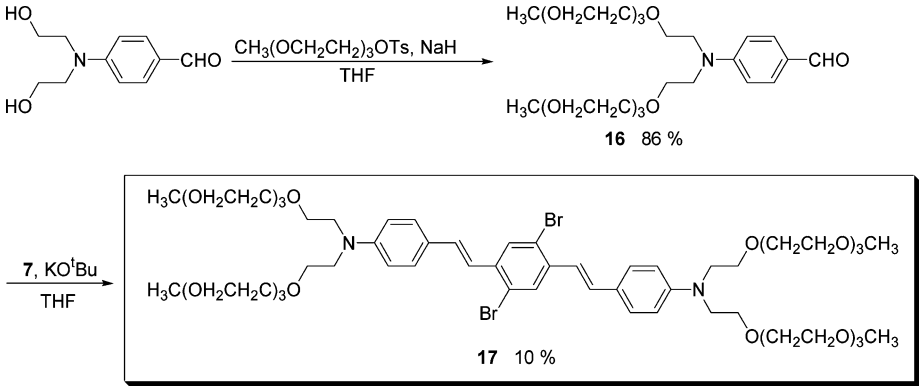

SCHEME 4. Synthesis of the Sulfonic Acid End-Capped OPV Using a HWE Strategy

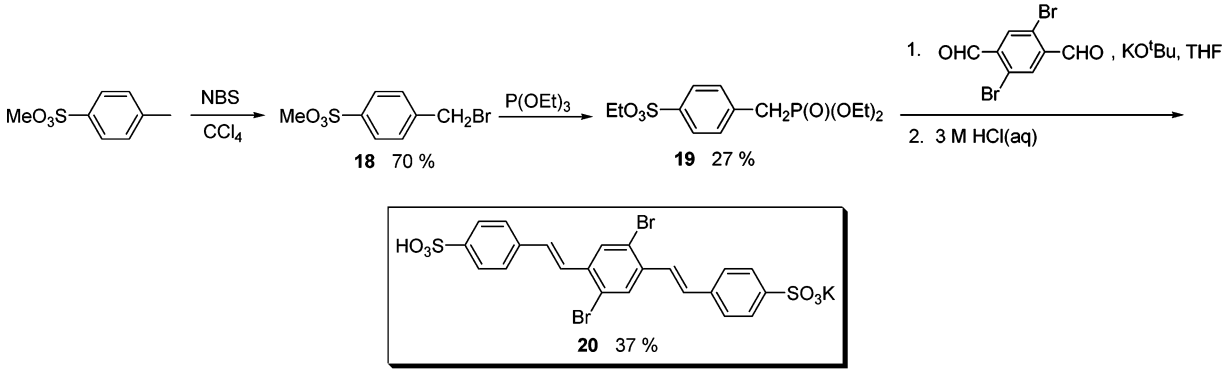

All of the MTEG-substituted benzaldehydes were made from commercially available hydroxy-substituted benzaldehydes, except 3,4,5-trihydroxy-benzaldehyde. To the best of our knowledge, only two methods have been reported for preparing this compound: (1) the seminal work of Rosenmund and co-workers on gallous acid,[35,36] and (2) a newer route from the acetyl-protected acid that proceeds by reduction to the alcohol with diborane, followed by reoxidation to the aldehyde with pyridinium dichromate.[37] In our work, an alternative to the Rosenmund reduction was attempted using $(Ph_3P)_2CuBH_4$ as the reducing agent. But this proceeded in only moderate yield (56%).

A more practical and atom-economical way of preparing the aldehyde without using chromic reagents is to reduce the acetyl-protected gallous acid to the alcohol with $BH_3{\cdot}Me_2S$, followed by reoxidation to the aldehyde using a Swern oxidation[38] (Scheme 2). The acetyl groups were then removed with sodium methoxide in methanol as described previously.[35,36] Going beyond the framework of our present work, it should be noted that the resultant trihydroxy-benzaldehyde is an important building block in the synthesis of certain dendrimers[39] and that many biologically active compounds contain a trihydroxy-functionalized aromatic ring.[40]

As outlined in Scheme 1, the MTEG-substituted OPVs were then prepared from the MTEG-substituted benzaldehydes using a HWE reaction with the diphosphonate ester **7**.

In addition to using MTEG groups directly attached to the terminal aryl rings of the OPV system, we also prepared OPV **17** with MTEG-substituted amino groups as outlined in Scheme 3. The yield of the HWE reaction for the preparation of **17** was relatively low, however. This is ascribed to the workup, where it was difficult to elute **17** from the chromatography column.

In one group of ionic OPV-based sensitizers, the goal was to use the anions of sulfonic acid moieties to impart water solubility. As shown in Scheme 4, one such acid was prepared by an HWE reaction between the phosphonate ester **19** and 2,5-dibromo-terephthalaldehyde. The phosphonate ester **19** was prepared by brominating toluene-4-sulfonic acid methyl ester and then converting the resultant 4-bromomethyl-benzenesulfonic acid methyl ester (**18**) into the phosphonate ester (**19**) using the Michaelis−Arbuzov reaction.[41] In this reaction, the methyl sulfonic ester transesterified forming the ethyl ester, which was later hydrolyzed during workup after the HWE reaction. The monopotassium salt of the sulfonic acid was isolated.

(35) Rosenmund, K. W.; Zetzsche, F. *Chem. Ber./Recl.* **1918**, *51*, 594−602.
(36) Rosenmund, K. W.; Pfannkuch, E. *Chem. Ber./Recl.* **1922**, *55*, 2357−2372.
(37) Schmidt, U.; Wild, J. *Liebigs Ann. Chem.* **1985**, *9*, 1882−1894.
(38) Mancuso, A. J.; Swern, D. *Synthesis* **1981**, *3*, 165−185.
(39) Brouwer, A. J.; Mulders, S. J. E.; Liskamp, R. M. J. *Eur. J. Org. Chem.* **2001**, *10*, 1903−1915.
(40) Ito, C.; Itoigawa, M.; Mishina, Y.; Tomiyasu, H.; Litaudon, M.; Cosson, J. P.; Mukainaka, T.; Tokuda, H.; Nishino, H.; Furukawa, H. *J. Nat. Prod.* **2001**, *64*, 147−150.
(41) Bhattacharya, A. K.; Thyagarajan, G. *Chem. Rev.* **1981**, *81*, 415−430.

SCHEME 5. Synthesis of the *N*-Methylated Benzothiazole Derivatives

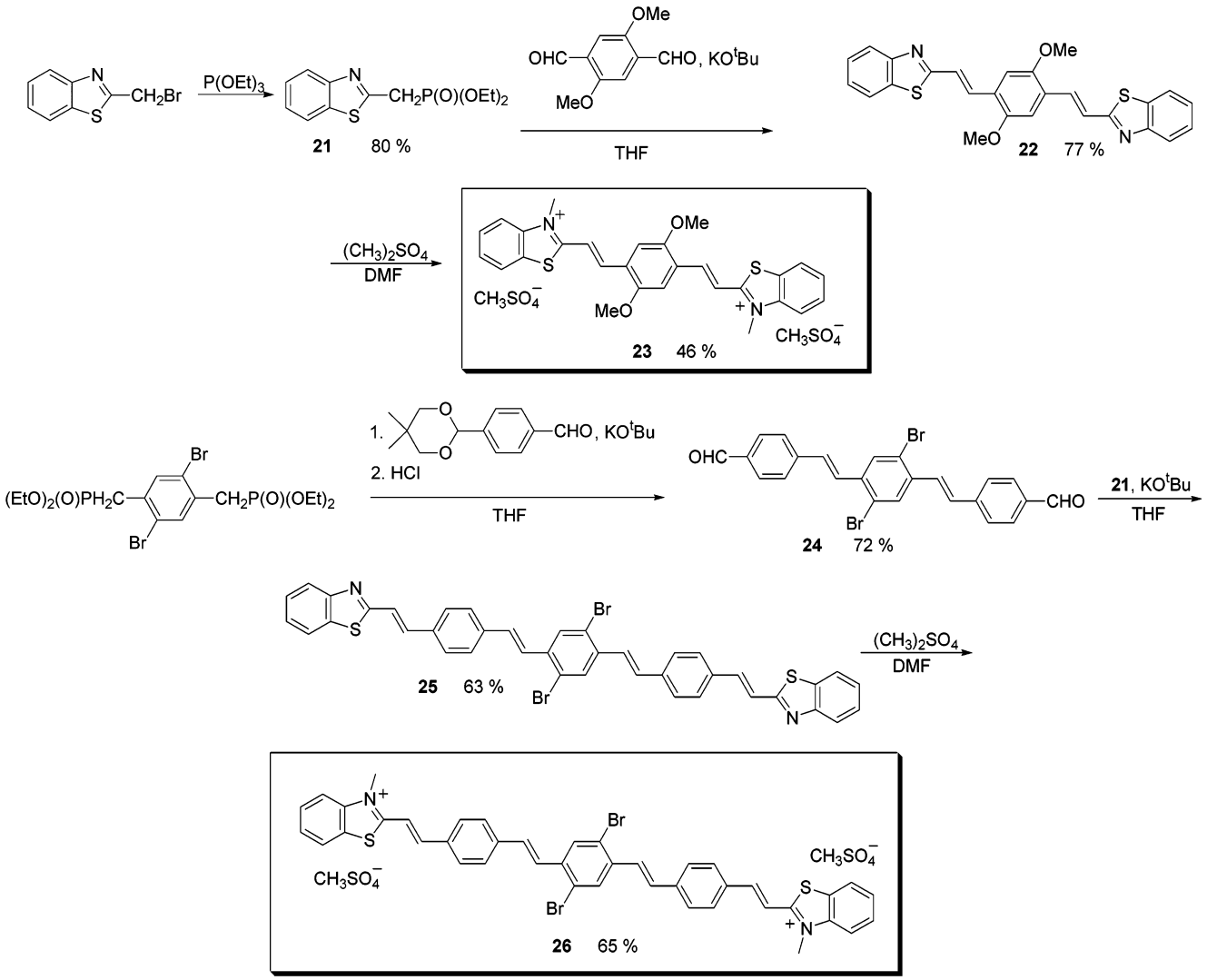

The typical way of introducing sulfonic acid functionalities on an aromatic ring is by direct sulfonation with HSO_3Cl or a reaction with SO_3 in concentrated sulfuric acid. These are not viable strategies for functionalizing acid-sensitive molecules. Our approach constitutes a mild method for introducing the sulfonic acid functionality. To the best of our knowledge, this is the first example of an HWE reaction involving a sulfonic acid-substituted phosphonate ester. Unfortunately, the sulfonic acid-derivatized OPV **20** turned out to be sparingly soluble in water. However, we did manage to get enough into solution in a 1 M sodium hydroxide solution to record an absorption spectrum.

Our quest to make ionic water-soluble OPV derivatives was more successful with the use of substituents based on positively charged salts of *N*-methyl-pyridinium, 1,1-dimethyl-piperazinium, and *N*-methyl-benzothiazolium moieties. An A−π−D−π−A architecture using methoxy groups as donors was employed in the design of the *N*-methyl-benzothiazolium derivative **23** (Scheme 5). Although initial attempts were made to condense *N*-methyl-benzothiazolium iodide with 2,5-dimethoxybenzene-1,4-dicarbaldehyde, we were unable to isolate **23** with iodide as the counterion using this approach. Benzothiazolium derivatives are normally prepared by a Knoevenagel condensation with a *N*-methyl-benzothiazolium salt, but problems are usually encountered with this strategy as two benzothiazole molecules can condense with one aldehyde.[42] Problems have also been reported with attempts to condense benzothiazole salts with ortho-substituted benzaldehydes.[42] All of these difficulties can be avoided by using the HWE methology illustrated in Scheme 5, and **22** was prepared by reacting 2,5-dimethoxybenzene-1,4-dicarbaldehyde with the phosphonate ester **21**. The *N*-methyl-benzothiazolium salt **23** was made by heating a solution of **22** with dimethyl sulfate in DMF.

In an attempt to prepare a sensitizer with a longer conjugated bridge between the terminal electron acceptors and one that would have a larger probability for intersystem crossing, we made **26** (Scheme 5). In this case, the aldehyde end-capped OPV (**24**) was prepared by reacting monoacetal protected terephthalaldehyde with **7** followed by hydrolysis of the acetal protecting groups during aqueous workup. Compound **25** was then prepared by reacting the dialdehyde **24** with the phosphonate ester **21**. The *N*-methyl-benzothiazolium salt **26**

(42) Jørgensen, M.; Krebs, F. C. *J. Org. Chem.* **2004**, *69*, 6688−6696.

SCHEME 6. Preparation of the Tetrabromo Phosphonate Ester (28)

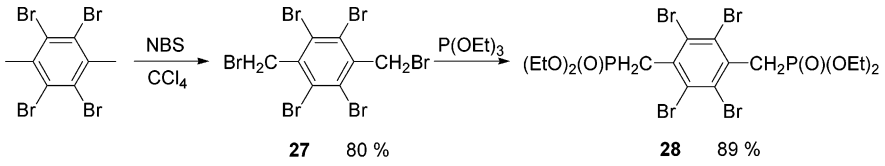

SCHEME 7. Synthesis of the Pyridinium OPV Salts

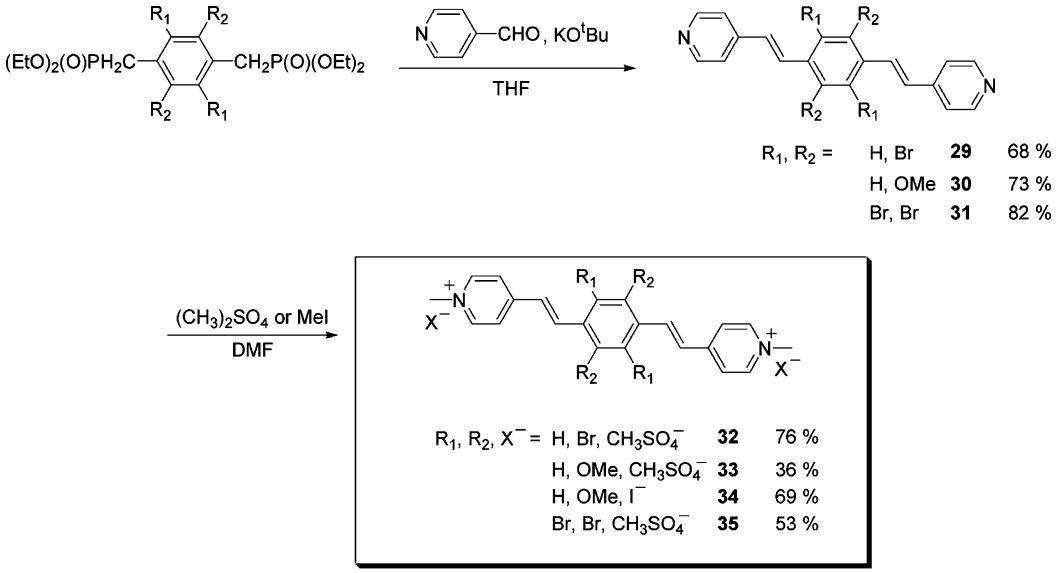

SCHEME 8. Preparation of a Water-Soluble 1,1-Dimethyl-piperazine Derivative (37)

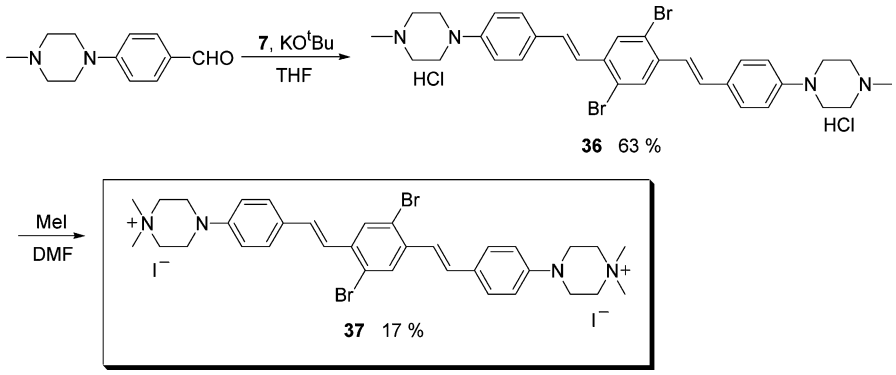

was likewise made by heating a solution of **25** with dimethyl sulfate in DMF.

The preparation of the pyridinium salts **32**, **33**, **34**, and **35** is outlined in Scheme 7. In these cases, reaction of the appropriate phosphonate ester with 4-pyridine-carboxaldehyde was followed by conversion to the *N*-methyl-pyridinium salt upon treatment with dimethyl sulfate in DMF. The tetrabromo phosphonate ester (**28**) used for making **31** was prepared as shown in Scheme 6. To investigate the effect of having a different counterion, in this case iodide, **30** was also treated with methyl iodide in a Menschutkin reaction[43] to yield **34**.

The free base **30** was obtained when the HWE reaction was quenched with water, whereas the dihydrochloride salt (**30·2HCl**) was obtained when the reaction was quenched with dilute hydrochloric acid. For **29** and **31**, however, only the free bases were isolated irrespective of whether the HWE reaction was quenched with water or dilute hydrochloric acid.

A crystal structure of **35** shows that the end methyl pyridinium rings are almost completely perpendicular to the tetrabromo-substituted center ring and that the double bonds are not coplanar with the center ring (Figure 1, the crystallographic data are presented in the Supporting Information).

For the cationic salts prepared in Schemes 5 and 7, the cation is an integral part of the chromophore. We also prepared a piperizinium derivative in an attempt to isolate the cation from the π-conjugated system of the sensitizer (Scheme 8). In this case, the HWE reaction was quenched with dilute hydrochloric acid and the dihydrochloride **36** was isolated. Interestingly, reaction of this dihydrochloride with methyl iodide yielded the 1,1-dimethyl-piperazinium salt (**37**). In principle, the Menschutkin reaction with methyliodide can result in the methylation of either of the two different amine func-

(43) Menschutkin, N. *Ber. Dtsch. Chem. Ges.* **1895**, *28*, 1398−1407.

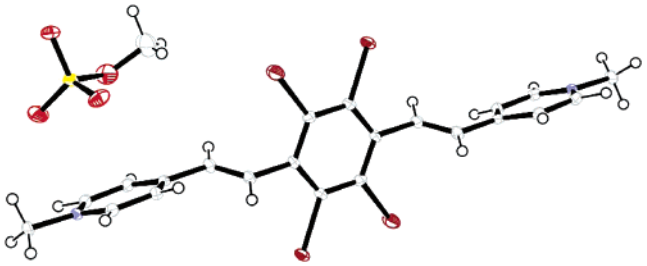

FIGURE 1. ORTEP-III plot of the crystal structure of **35** (50% ellipsoids) including one $CH_3SO_4^-$ counterion. The end-methyl pyridinium rings are almost perpendicular to the center ring. The connecting double bonds are also not in the same plane as the center ring.

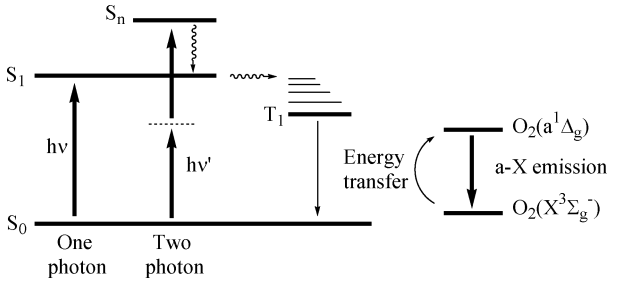

FIGURE 2. Jablonski diagram illustrating the triplet-sensitized production of singlet oxygen in both one- and two-photon excitation schemes.

tionalities in **36**. The ^{1}H- and ^{13}C NMR spectra obtained, however, showed only one type of *N*-methyl group in accordance with what is shown for **37** in Scheme 8. Methylation of **36** with dimethyl sulfate was attempted, but the product isolated was not stable upon exposure to air (i.e., with $CH_3SO_4^-$ as the counterion, the product isolated by filtration rapidly changed color from yellow to brown and then to black).

Photophysical Characterization. The photophysical processes that occur upon both one- and two-photon irradiation of a singlet oxygen sensitizer are shown in Figure 2. For centrosymmetric molecules such as ours, selection rules dictate that the state initially populated upon one-photon irradiation is different from that initially populated upon two-photon irradiation.[44−46] However, we assume that, irrespective of the excitation method and which state is populated first, Kasha's rule[47] will hold and that all subsequent photophysics and photochemistry originate from one common state: the vibrationally relaxed, lowest-energy excited singlet state, S_1. As such, measurements of fluorescence and singlet oxygen yields performed under one-photon conditions can be compared to those obtained under two-photon conditions.

Although singlet oxygen can be produced upon oxygen quenching of S_1,[48] the S_1 lifetime in most molecules is generally so short as to render this bimolecular process improbable. Rather, singlet oxygen is more efficiently produced upon oxygen quenching of the longer-lived triplet state of the sensitizer. As such, singlet oxygen quantum yields, ϕ_Δ, are generally the largest for molecules that have large quantum yields of intersystem crossing and, correspondingly, small quantum yields of fluorescence, ϕ_f. Pertinent photophysical data for some of the compounds prepared in the present work are summarized in Table 1.

TABLE 1. Photophysical Properties of Selected OPVs[a]

compd	solvent	λ_{max}^{abs} (nm)	log ϵ[b]	λ_{max}^{f} (nm)	τ_s (ns)	ϕ_f[c]	ϕ_Δ[c]
8	toluene	354	4.37	426, 450	0.2	0.12	0.33
9	toluene	370	4.62	430, 454	0.2	0.11	0.35
10	toluene						0.32
	water						0.20
11	toluene	364		443, 462		0.19	0.26
	water	348		483		0.04	0.14
12	toluene	352		415, 436			0.18
	water	337		442			0.10
13	toluene	362					0.35
	water	347					0.14
17	toluene	335, 426		496, 526		0.16	0.33
	water	352, 418		557		0.04	0.11[d]
20	toluene	338	3.67	413, 438	0.3	0.12	0.22
	1 M NaOH	280					
23	water	491	4.65	639	1.9	0.18	0.01
		395	4.51				
26	water	509[e]		723[e]			
30	toluene	397	4.48	457	1.9	0.01	0.31
		326	4.38				
32	water	360	4.49	466		0.01	0.03
33	water	446	4.60	604	1.5	0.14	0.02
		360	4.48				
34	water	445	4.82	604	1.6	0.14	0.02
		358	4.71				
35	water	315	4.53	438		0.00	0.00
37	water	364	4.39	569	1.0	0.07	0.00

[a] Singlet oxygen quantum yield, ϕ_Δ; one-photon absorption band maximum, λ_{max}^{abs}; molar extinction coefficient, ϵ; fluorescence band maximum, λ_{max}^{f}; fluorescence quantum yield, ϕ_f; S_1 lifetime, τ_s. [b] ϵ has the units cm^{-1} M^{-1}. [c] Errors are ±10%. [d] Measured in D_2O. [e] Broad bands.

A. Absorption and Fluorescence Spectra. All the MTEG-substituted OPV molecules (**8**−**13**) and the OPV salts with two bromine atoms on the central aromatic ring (**20**, **32**, and **37**) have a single broad one-photon absorption band between ~300 and 400 nm (Figure 3a,d). On the other hand, the compounds with comparatively strong electron-donating methoxy groups on the central aromatic ring (i.e., **23**, **33**, and **34**) have a second discrete absorption band whose maximum is red-shifted with respect to that of the first band (Figure 3b). We assign this second band to a transition that populates a comparatively low-lying CT state. It was difficult to dissolve the more extensively conjugated *N*-methyl-benzothiazolium derivative **26** in water, and the absorption maximum reported in Table 1 for this compound may be that for an aggregated species. This is consistent with the rather broad spectral profile observed for **26**.

The piperazine salt **37** has an absorption maximum (364 nm) very similar to that of the *N*-methylpyridyl salt

(44) McClain, W. M. *Acc. Chem. Res.* **1974**, *7*, 129−135.
(45) McClain, W. M. *J. Chem. Phys.* **1971**, *55*, 2789−2796.
(46) Monson, P. R.; McClain, W. M. *J. Chem. Phys.* **1970**, *53*, 29−37.
(47) Gilbert, A.; Baggott, J. *Essentials of Molecular Photochemistry*; CRC Press: Boca Raton, FL, 1991.
(48) Dobrowolski, D. C.; Ogilby, P. R.; Foote, C. S. *J. Phys. Chem.* **1983**, *87*, 2261−2263.

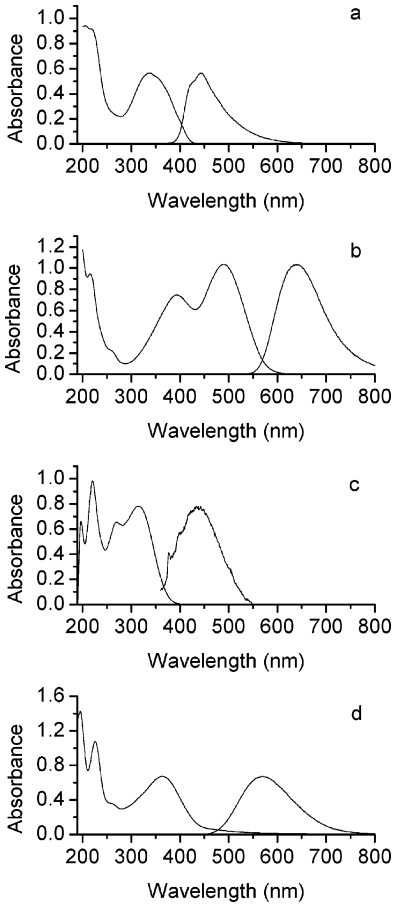

FIGURE 3. Representative examples of absorption and fluorescence spectra recorded in H_2O. (a) **12**. (b) **23**. (c) **35**. (d) **37**.

32 (360 nm). In contrast, the free-base amino analogue **17** has an absorption maximum at 418 nm. We infer from these data that the lone-pair electrons on the phenyl-substituted nitrogens in **37**, assumed to be part of the chromophore, are in fact decoupled from the π-system. Indeed, as outlined below in our discussion of singlet oxygen yields, our data are consistent with a π-system in **37** characterized by an appreciable amount of positive charge. These observations suggest that we have failed in our attempt to isolate the terminal cationic site from the π-system in **37**.

Fluorescence data were also recorded for the compounds prepared (Table 1, Figure 3). Even though quantum yields of fluorescence were very small in many cases (e.g., $\phi_f \approx 0$ for **35**), we were able to record data with appreciable signal-to-noise ratios (e.g., see spectrum for **35** in Figure 3c). With compound **23**, for which we recorded a distinct absorption band assigned to a CT transition (vide supra), the same fluorescence spectrum was obtained irrespective of the irradiation wavelength (Figure 3b). More specifically, when monitoring emission at 639 nm, the excitation spectrum of **23** was identical to the absorption profile independently recorded. These data are consistent with a process in which emission in **23** occurs from the low-lying CT state.

B. Singlet Oxygen Quantum Yields. The singlet oxygen quantum yields, ϕ_Δ, reported in the present work were obtained in time-resolved experiments by comparing the intensity of the 1270 nm singlet oxygen phosphorescence produced upon one-photon irradiation of the given sensitizer to that obtained upon one-photon irradiation of a standard sensitizer (phenalenone with $\phi_\Delta = 1.00 \pm 0.05$[49]). The concentrations of the dyes used were adjusted such as to yield an absorbance at the irradiation wavelength of ~0.2−0.3. In general, this corresponds to [dye] $< 2 \times 10^{-5}$ M. With respect to the experiments performed in water, we ascertained that the Lambert−Beer relationship was valid over a range of dye concentrations whose upper limit exceeded the concentration used for the quantum yield measurements (i.e., absorbance was linearly dependent on dye concentration). Thus, dye aggregation does not appear to be a problem for the molecules studied.

In a triplet state photosensitized process, the evolution of singlet oxygen in time is described in the sequence of reactions shown in Scheme 9.

SCHEME 9. Evolution of Singlet Oxygen in a Triplet Photosensitized Process[a]

$$O_2(X^3\Sigma_g^-) \xrightarrow[T_1]{k_{form}} O_2(a^1\Delta_g) \xrightarrow{k_{decay}} O_2(X^3\Sigma_g^-)$$

[a] Singlet oxygen ($O_2(a^1\Delta_g)$) is formed in a collision between the photosensitizer triplet state and ground state oxygen ($O_2(X^3\Sigma_g^-)$). Thereafter, singlet oxygen is removed from the system by a number of processes (i.e., chemical reaction, bimolecular quenching, solvent-induced photophysical decay). For our present purposes, we identify only one of these channels: decay to ground state oxygen with a rate constant k_{decay}.

On the basis of the kinetic sequence shown in Scheme 9, the concentration of singlet oxygen will evolve in time according to:

$$[O_2(a^1\Delta_g)]_t = \frac{k_{form}[O_2(X^3\Sigma_g^-)]}{k_{decay} - k_T}[T_1]_0(\exp(-k_T t) - \exp(-k_{decay} t)) \quad (1)$$

where k_T is the rate constant that expresses all channels for the decay of the photosensitizer triplet state, including the oxygen-dependent bimolecular channel $k_{form}[O_2(X^3\Sigma_g^-)]$, and $[T_1]_0$ is the initial concentration of sensitizer triplet state. In a typical aqueous system, the rate constants k_{decay} and k_T will be roughly equal,[22] and as a consequence, the time evolution of the singlet oxygen signal should appear as the difference of two exponential functions, showing distinct rising and falling components. In Figure 4, we show time-resolved singlet oxygen phosphorescence signals produced upon irradiation of **10** in water.

Upon irradiation of the sensitizer at comparatively low powers (e.g., less than ~1 mW or 1 μJ/pulse with our femtosecond system), the data obtained correspond to those expected on the basis of eq 1 (Figure 4a). Moreover, in a fit of eq 1 to the data, we obtain a singlet oxygen lifetime (i.e., $1/k_{decay}$) that is consistent with that expected for H_2O (~3.5 μs[50,51]). Upon irradiation of **10** at higher laser powers (greater than ~1 mW or 1 μJ/pulse with our femtosecond system), the time-resolved singlet oxygen phosphorescence signal shows an increased deviation

(49) Schmidt, R.; Tanielian, C.; Dunsbach, R.; Wolff, C. *J. Photochem. Photobiol., A* **1994**, *79*, 11−17.

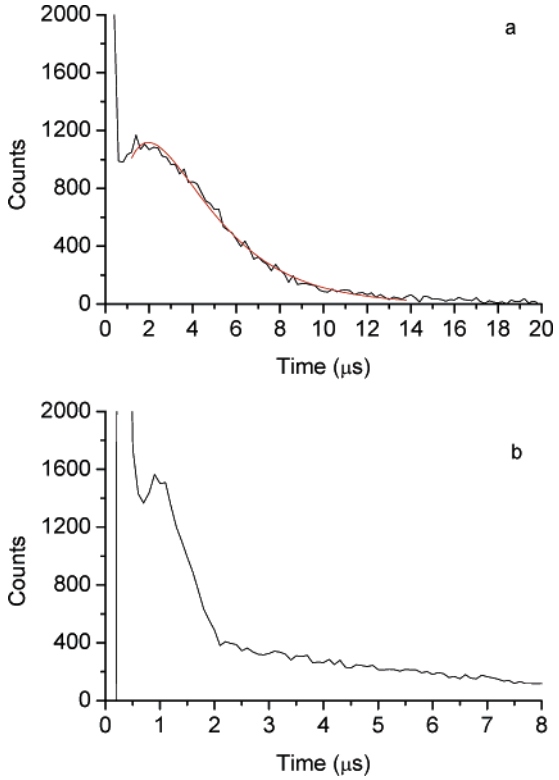

FIGURE 4. Time-resolved 1270 nm phosphorescence signal from singlet oxygen in H_2O using **10** as the photosensitizer. Data were recorded after pulsed femtosecond irradiation of the sensitizer, and singlet oxygen was monitored in a single photon counting experiment. (a) Low laser power, i.e., 0.4 mW or 0.4 μJ/pulse. (b) High laser power, i.e., 4 mW or 4 μJ/pulse. The intense "spike" preceding the singlet oxygen signal is due to a combination of sensitizer fluorescence, scattered laser light, and luminescence from the optics used.

from first-order single-exponential decay kinetics (Figure 4b). Such behavior is commonly observed and has been interpreted to reflect the photoinduced production of a transient species that can quench singlet oxygen and whose lifetime is somewhat shorter than that of singlet oxygen.[28,52] On the basis of these latter observations, all singlet oxygen quantum yields were obtained using low laser powers. (As an aside, it is important to note that, in a typical two-photon experiment, where the sample may be exposed to comparatively high laser powers, the number of photons actually absorbed is significantly less than that in the one-photon case. As such, all of the two-photon-induced singlet oxygen signals we have observed thus far in our work decay with single-exponential kinetics.)

For all sensitizers in which electron-withdrawing ionic groups are an integral part of the chromophore, a comparatively small yield of singlet oxygen was obtained. In contrast, the non-ionic, MTEG-substituted sensitizers produce singlet oxygen in greater yield. For the latter molecules, an appreciable solvent effect on ϕ_Δ was observed, indicating that singlet oxygen is more efficiently produced in toluene than it is in the more polar solvent water. Although this observation could reflect a number of solvent-dependent phenomena (vide infra), the data are at least consistent with the thesis that CT character in a sensitizer and/or sensitizer−oxygen complex can adversely affect singlet oxygen yields by providing an independent pathway for the deactivation of sensitizer excited states that competes with energy transfer to $O_2(X^3\Sigma_g^-)$.[28,29] Keeping the framework of this model in mind, we now focus on several specific points.

Within the MTEG-substituted series, the singlet oxygen quantum yields consistently reflect the substitution pattern of the pendant ether. Thus, for compounds in which the alkoxy groups are ortho and/or para to the vinyl moiety, the singlet oxygen yield is comparatively large. In contrast, for the compounds in which the alkoxy groups are meta to the vinyl moiety, the singlet oxygen yield is noticeably smaller. These observations are consistent with the expectation that, in contrast to the effect of withdrawing electron density from the chromophore, electron-donating groups cause, through resonance effects, an increase in ϕ_Δ.

It is clear that, for this particular series of OPV-based sensitizers, addition of positively charged electron-withdrawing substituents to each end of the π-system adversely affects the singlet oxygen yield. This is seen not only in the comparison between the MTEG- and ionic *N*-methylated species, but in the comparison between the ionic *N*-methylated species and the corresponding non-methylated amines. For example, for the pyridine-terminated OPV **30**, $\phi_\Delta \approx 0.3$, whereas for the corresponding *N*-methylpyridinium-terminated OPVs **33** and **34**, $\phi_\Delta \approx 0$. Similarly, ϕ_Δ values for the amino-terminated OPV **17** are noticeably larger than ϕ_Δ values for the corresponding *N*-methylated compounds **32** and **37**. Indeed, the observation of $\phi_\Delta \approx 0$ for the *N*-methylpiperazine (**37**) suggests an appreciable 1,4-transannular interaction in the terminal piperazinyl groups that, in turn, couples positive charge onto the π-framework.

Singlet oxygen yields can be influenced by many features of a given sensitizer, only one of which is the extent of CT character. The latter can manifest its effects in the sensitizer−oxygen contact complex that necessarily precedes singlet oxygen formation.[28−30,53,54] Alternatively, prior to any interaction with oxygen, CT character in the sensitizer can influence the energy, yield, and lifetime of the sensitizer triplet state,[55] all of which can, likewise, ultimately be reflected in the singlet oxygen yield.

C. Sensitizer Triplet State Yields and Lifetimes. To provide a more satisfying explanation for the singlet oxygen yields reported in Table 1, it is necessary to examine aspects of the triplet states of the respective sensitizers. For example, the relative energy of the sensitizer triplet state will influence the efficiency of singlet oxygen production,[30] and this energy is certainly expected to change upon methylation of a nitrogen atom whose lone-pair electrons are an integral part of the chromophore. This phenomenon could certainly influence

(50) Egorov, S. Y.; Kamalov, V. F.; Koroteev, N. I.; Krasnovsky, A. A.; Toleutaev, B. N.; Zinukov, S. V. *Chem. Phys. Lett.* **1989**, *163*, 421−424.
(51) Schmidt, R.; Afshari, E. *Ber. Bunsen-Ges. Phys. Chem.* **1992**, *96*, 788−794.
(52) Gorman, A. A.; Rodgers, M. A. J. *J. Am. Chem. Soc.* **1986**, *108*, 5074−5078.
(53) Stevens, B.; Small, R. D. *Chem. Phys. Lett.* **1979**, *61*, 233−238.
(54) Garner, A.; Wilkinson, F. *Chem. Phys. Lett.* **1977**, *45*, 432−435.
(55) McGlynn, S. P.; Azumi, T.; Kinoshita, M. *Molecular Spectroscopy of the Triplet State*; Prentice Hall: Englewood Cliffs, NJ, 1969.

SCHEME 10. Kinetic Scheme for the Photosensitized Production of Singlet Oxygen

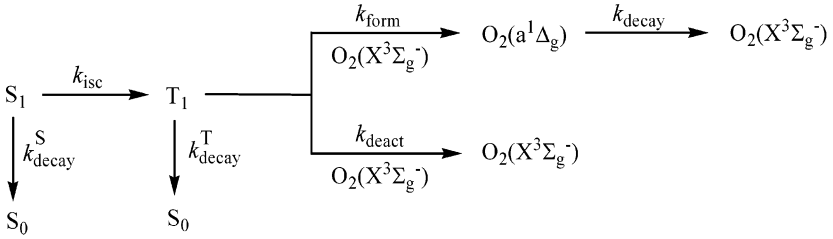

$\tau_T = \frac{1}{k^T_{decay}}$ is the inherent, oxygen-independent lifetime of the triplet state

$k_q^T = k_{form} + k_{deact}$ is the overall rate constant for O_2 quenching of the triplet state

$f_T = \frac{k_q^T[O_2(X^3\Sigma_g^-)]}{k_q^T[O_2(X^3\Sigma_g^-)] + k^T_{decay}}$ is the fraction of triplet states quenched by O_2

$S_\Delta = \frac{k_{form}}{k_{form} + k_{deact}}$ is the fraction of O_2 quenching events that result in $O_2(a^1\Delta_g)$

the singlet oxygen yields observed for **30** and **33** as well as **37**, for example. Sensitizer triplet yields and lifetimes will likewise have a direct effect on singlet oxygen production, and we set out to examine these issues in detail for several of our compounds.

When comparing photophysical data obtained in toluene with those obtained in water, it is essential to account for the comparatively low solubility of oxygen in the latter solvent.[56] Specifically, differences in the concentration of ground state oxygen, $O_2(X^3\Sigma_g^-)$, in these solvents can have a pronounced effect on the respective yields of singlet oxygen, particularly if the inherent lifetime of the sensitizer triplet state is comparatively short. To facilitate discussion of this point, and related material, we refer to the kinetic model shown in Scheme 10.

Compound 17. Upon irradiation of compound **17** in water and toluene solutions, the fluorescence intensities and lifetimes obtained in oxygen-saturated solutions were the same as those in nitrogen-saturated solutions. These data indicate that oxygen does not quench the S_1 state, an observation that is consistent with the comparatively short singlet state lifetimes of these OPV molecules (Table 1).

Upon 355 nm pulsed laser irradiation of **17** in toluene, we observed a transient absorption signal with λ_{max} at 630 nm. This signal decayed in a first-order process, yielding a lifetime of 2.9 ± 0.1 μs in a nitrogen-saturated solution (Figure 5a). In an air-saturated solution, the lifetime of this transient decreased to 0.18 ± 0.01 μs (Figure 5b). With an oxygen concentration of 1.7×10^{-3} M in air-saturated toluene,[56] these data yield a rate constant of $(3.1 \pm 0.2) \times 10^9$ M^{-1} s^{-1} for oxygen-induced deactivation of the transient. These oxygen-dependent results that yield a quenching rate constant approximately 10 times smaller than the diffusion-limited rate constant are consistent with assigning this transient signal to the triplet state of **17**.[57]

The initial absorbance of this triplet signal (i.e., at time = 0) was independent of oxygen. This observation is consistent with an S_1 lifetime in **17** that is short enough to preclude quenching by oxygen (vide supra). Most importantly, however, the lifetime of the triplet state in the absence of oxygen, $\tau_T = 2.9 \pm 0.1$ μs, is likewise short, certainly in comparison to triplet lifetimes for many other organic molecules.[58] This latter observation was verified in an independent photoacoustic experiment (Figure 6).

For photoacoustic experiments performed against a calibrated reference standard, one can accurately quantify the fraction of "fast" heat released by a given compound, α, and distinguish this from heat released over longer periods of time (i.e., "slow" heat release).[59,60] For our experiment performed in the presence of oxygen, fast heat release derives from S_n and T_n deactivation in the sensitizer, whereas slow heat release reflects $O_2(a^1\Delta_g)$ deactivation (see Scheme 10 and Figure 2). For compound **17** in air-saturated toluene, the photoacoustic data yield $\alpha = 0.77 \pm 0.06$. Using all of the photophysical parameters determined thus far for this particular system, we found that the calculated expected value of α is 0.80 ± 0.02.[61] This independent exercise confirms the accuracy of data reported in Table 1.

Upon 355 nm pulsed laser irradiation of **17** in water, we were unable to detect a transient absorption signal that could be assigned to the triplet state. From photo-

(56) *IUPAC Solubility Data Series. Volume 7: Oxygen and Ozone*; Battino, R., Ed.; Pergamon Press: Oxford, 1981.

(57) Gijzeman, O. L. J.; Kaufman, F.; Porter, G. *J. Chem. Soc., Faraday Trans. 2* **1973**, *69*, 708−720.

(58) Carmichael, I.; Hug, G. L. In *CRC Handbook of Organic Photochemistry*; Scaiano, J. C., Ed.; CRC Press: Boca Raton, FL, 1989; Vol. 1, pp 369−403.

(59) Heihoff, K.; Redmond, R. W.; Braslavsky, S. E.; Rougee, M.; Salet, C.; Favre, A.; Bensasson, R. V. *Photochem. Photobiol.* **1990**, *51*, 635−641.

(60) Braslavsky, S. E.; Heibel, G. E. *Chem. Rev.* **1992**, *92*, 1381−1410.

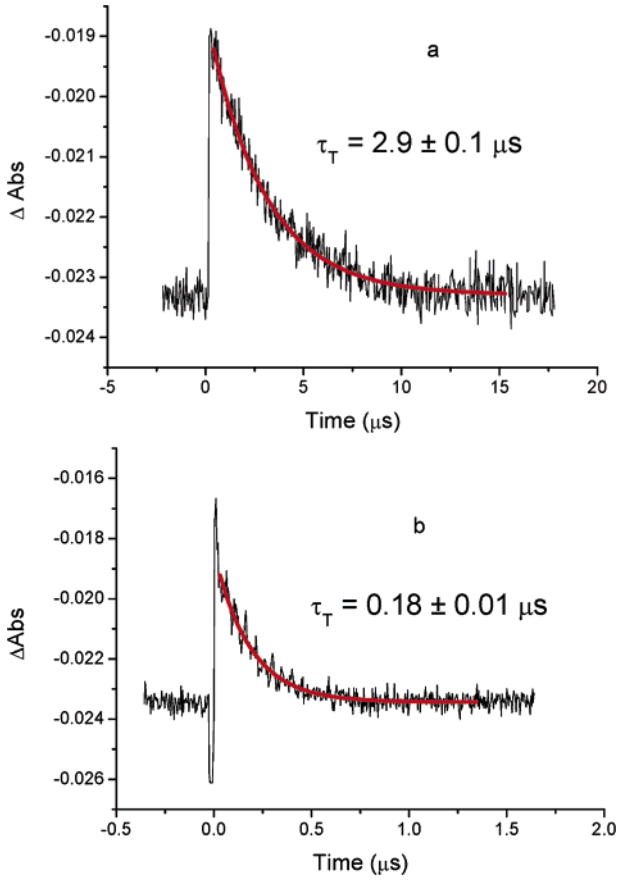

FIGURE 5. Transient absorption signals recorded at 630 nm upon 355 nm pulsed laser irradiation of compound **17** in toluene. (a) Nitrogen-saturated solution. (b) Air-saturated solution.

acoustic measurements, however, we obtained $\alpha = 0.94 \pm 0.08$. Using the photophysical parameters independently obtained for this system (Table 1),[62] we calculated an expected value of 0.95 ± 0.01 for α.

We now examine the relative magnitudes of the singlet oxygen quantum yield for compound **17** in water and toluene.

From Table 1, we see that

$$\frac{\phi_\Delta^{\text{water}}}{\phi_\Delta^{\text{toluene}}} = \frac{0.11 \pm 0.01}{0.33 \pm 0.03} = 0.33 \pm 0.05 \qquad (2)$$

From Scheme 10, we see that, in the triplet sensitized production of singlet oxygen,

$$\phi_\Delta = \phi_T f_T S_\Delta \qquad (3)$$

(61) The following expression was used to calculate α, the fraction of heat released as "fast" heat: $E_{\text{laser}}(1-\alpha) = \phi_f E_f + \phi_\Delta E_\Delta \exp(-\tau_a/\tau_\Delta)$ where E_{laser} is the energy imparted by the pulsed laser used to irradiate the system at 355 nm (337 kJ/mol), ϕ_f is the quantum efficiency of fluorescence (0.16), E_f is the energy of the fluorescent state (241 kJ/mol, obtained from λ_{max} fluorescence), ϕ_Δ is the quantum yield of singlet oxygen (0.33), E_Δ is the excitation energy of singlet oxygen (94 kJ/mol), τ_Δ is the lifetime of singlet oxygen in toluene (30 μs), and τ_a is the effective acoustic transit time in toluene (500 ns). The latter parameter is determined by the laser beam radius and the speed of sound in toluene.

(62) In this case, the following parameters were used in the calculation: $\phi_f = 0.04$, $E_f = 215$ kJ/mol, $\phi_\Delta = 0.11$, $\tau_\Delta = 4$ μs.

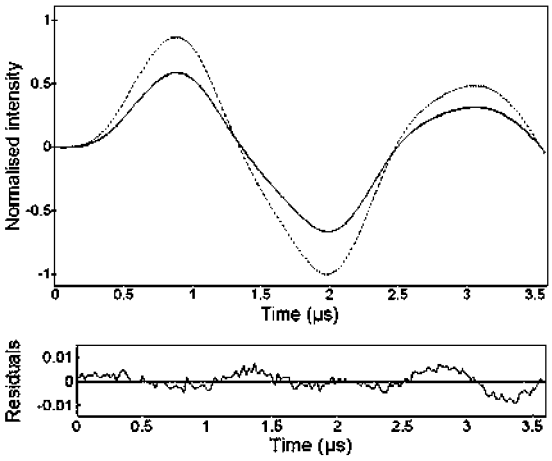

FIGURE 6. (Top) Photoacoustic signal observed after pulsed laser irradiation of **17** (solid line), and independently, the signal observed from the reference standard, 2-hydroxybenzophenone (dashed line). Superimposed on, and indistinguishable from, the data from **17** is a simulated acoustic signal obtained using a time constant for fast heat release of 1 ns and a time constant for slow heat release of 2.8 μs. The latter is consistent with the triplet lifetime obtained in the time-resolved optical absorption measurements (Figure 5a). (Bottom) Residuals plot for the difference between the simulated and actual data on **17**. Data were recorded in nitrogen-saturated toluene.

where ϕ_T is the triplet quantum yield. Thus,

$$\frac{\phi_\Delta^{\text{water}}}{\phi_\Delta^{\text{toluene}}} = \frac{\phi_T^{\text{water}} f_T^{\text{water}} S_\Delta^{\text{water}}}{\phi_T^{\text{toluene}} f_T^{\text{toluene}} S_\Delta^{\text{toluene}}} \qquad (4)$$

We ascertained that, in toluene, the inherent triplet lifetime of **17** in the absence of oxygen, τ_T, is 2.9 μs. Moreover, the rate constant for oxygen quenching of the triplet state of **17** is 3.1×10^9 M^{-1} s^{-1}. If we assume that these values are equally valid in water, and given that $[O_2]_{\text{toluene}} = 1.73$ mM and $[O_2]_{\text{water}} = 0.278$ mM in air-saturated solutions,[56] we can use the expression shown in Scheme 10 to quantify the relative fraction of triplet states quenched by oxygen, f_T, in these respective solvents (eq 5).

$$\frac{f_T^{\text{water}}}{f_T^{\text{toluene}}} = \frac{0.71 \pm 0.08}{0.94 \pm 0.08} = 0.76 \pm 0.11 \qquad (5)$$

Substituting eq 5 into eqs 2 and 4 yields

$$\frac{\phi_T^{\text{water}} S_\Delta^{\text{water}}}{\phi_T^{\text{toluene}} S_\Delta^{\text{toluene}}} = 0.44 \pm 0.08 \qquad (6)$$

Thus, taking into account the "trivial" effect of solvent-dependent changes in the oxygen concentration, we nevertheless find that the change in solvent from toluene to water has a pronounced adverse effect on the efficiency with which compound **17** can produce singlet oxygen. This decrease in production efficiency derives from solvent-dependent changes in two parameters, ϕ_T and S_Δ. Thus, with the change from a nonpolar to polar solvent, the changes observed in the singlet oxygen yield remain consistent with those expected for a solvent-dependent

increase in the extent of CT character, both in the sensitizer itself as well as in the sensitizer−oxygen complex.

Compound 11. Upon 355 nm pulsed laser irradiation of **11** in toluene, we observed a transient absorption signal with λ_{max} at 580 nm. This signal decayed in a first-order process, yielding a lifetime of 560 ± 30 ns in a nitrogen-saturated solution. In an air-saturated solution, the lifetime of this transient decreased to 160 ± 8 ns. With an oxygen concentration of 1.7×10^{-3} M in air-saturated toluene,[56] these data yield a rate constant of $(2.6 \pm 0.2) \times 10^9$ M^{-1} s^{-1} for oxygen-induced deactivation of the transient. These results are consistent with assigning this transient signal to the triplet state of **11**.

In a photoacoustic study of **11** in toluene, we obtained a value for "fast" heat release, α, of 0.77 ± 0.06. Using data in Table 1, we calculated an expected value of α = 0.77 ± 0.02. Thus, once again, the photoacoustic experiment independently confirms our optical data.

The comparatively short inherent triplet lifetime of **11** means that, in this case, the yield of singlet oxygen produced from the triplet state will be particularly sensitive to the effects of a solvent-dependent change in oxygen concentration. Once again, if we assume that the values of τ_T and k_q^T obtained for **11** in toluene are equally valid in water, and given that $[O_2]_{toluene} = 1.73$ mM and $[O_2]_{water} = 0.278$ mM in air-saturated solutions,[56] we obtain

$$\frac{f_T^{water}}{f_T^{toluene}} = \frac{0.29 \pm 0.04}{0.72 \pm 0.04} = 0.40 \pm 0.06 \qquad (7)$$

This result indicates that, indeed, differences in oxygen solubility have a pronounced effect on the fraction of compound **11** triplet states quenched by oxygen.

In this light, when we consider the ratio of singlet oxygen quantum yields obtained for compound **11** in these respective solvents,

$$\frac{\phi_\Delta^{water}}{\phi_\Delta^{toluene}} = \frac{0.14 \pm 0.01}{0.26 \pm 0.03} = 0.54 \pm 0.08 \qquad (8)$$

the relative effect of the change in solvent from toluene to water on the product $\phi_T S_\Delta$ is comparatively small for compound **11**. It is important to keep in mind, however, that the origin of this solvent effect ultimately derives from the uniquely short triplet lifetime of compound **11**. As already discussed, this in itself could be a consequence of a number of factors, including the extent of CT character in the molecule.

Compound 32. Recall that this molecule is a pyridinium salt, and the expectation is that that there is an appreciable amount of CT character in the system. Upon 355 nm pulsed laser irradiation of **32** in water, we observed a transient absorption signal with λ_{max} at 550 nm. This signal decayed in a first-order process, yielding a lifetime of 160 ± 8 ns in a nitrogen-saturated solution (Figure 7). In an air-saturated solution, the lifetime obtained was 150 ± 8 ns (Figure 7). These data yield a rate constant of 1.5×10^9 M^{-1} s^{-1} for the oxygen-induced deactivation of the transient (the errors on this number are large, however, because the calculation involves taking the difference between two large and similar numbers). On this basis, we assign this signal to the triplet state of **32**.

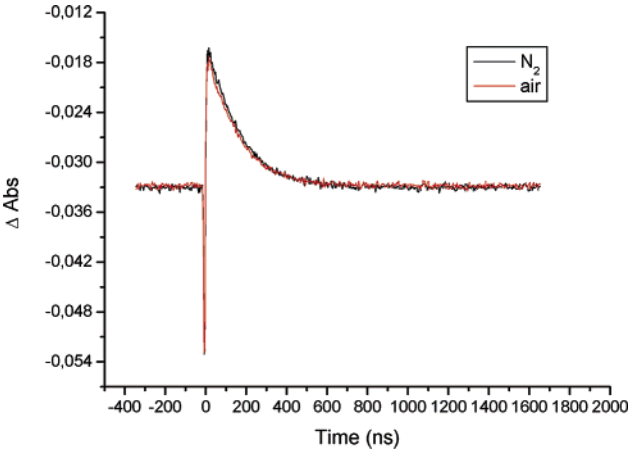

FIGURE 7. Transient absorption signals recorded at 550 nm upon 355 nm pulsed laser irradiation of compound **32** in water under both nitrogen- and air-saturated conditions.

The assignment of the rapidly decaying optical signal in Figure 7 to the triplet state is also consistent with the photoacoustic data recorded for this compound. Specifically, we obtain an experimental α value of 1.00 ± 0.05 and a calculated α value of 0.98 ± 0.02, indicating that essentially all the energy absorbed upon irradiation of **32** is released as "fast" heat. This result is in keeping with the fact that this molecule does not produce singlet oxygen in appreciable yield ($\phi_\Delta = 0.03$) nor does it fluoresce ($\phi_f = 0.01$).

The data obtained from compound **32** further reinforce our working hypothesis that substantial CT character in a given molecule can contribute to rapid nonradiative deactivation channels that compete with channels that eventually result in the production of singlet oxygen.

D. Sensitizer Stability. Although the water-soluble MTEG-substituted molecules produce singlet oxygen in moderate yields, these molecules were unfortunately not particularly stable upon irradiation in aerated H_2O. This is illustrated in Figure 8 with data recorded from **11** and **17**. In both cases, the degradation reactions involved appear to shorten the chromophore as seen by a decrease in the intensity of the longest wavelength absorption band. Moreover, distinct isosbestic points in the spectra indicate that, under the conditions of these experiments, only one degradation product is formed in each case. Similar behavior has been observed by Strehmel et al.[63] upon irradiation of other OPV systems.

Despite the apparent similarities in the data shown in Figure 8, the kinetics of degradation for **11** and **17** were different. It is important to first note that quantifying the kinetics of self-sensitized decay reactions can be complicated. Specifically, even over comparatively short periods of irradiation, the species absorbing light at a given wavelength can change, and in turn, different reactions can come into play.

With this caveat in mind, we note that the overall rate for photoinduced changes in a solution of **11** was slightly

(63) Strehmel, V.; Sarker, A. M.; Lahti, P. M.; Karasz, F. E.; Heydenreich, M.; Wetzel, H.; Haebel, S.; Strehmel, B. *ChemPhysChem* **2005**, *6*, 267−276.

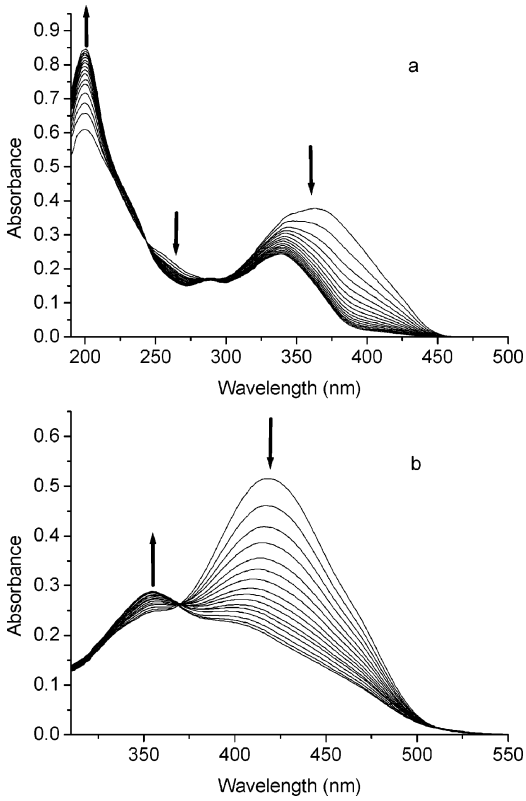

FIGURE 8. UV−vis absorption spectra of two MTEG-substituted sensitizers recorded as a function of elapsed exposure to 400 nm light in aerated H_2O (CW laser operated at 30 mW, irradiated spot size ~5 mm in diameter). Arrows on the respective spectra indicate whether the absorbance increases (up arrow) or decreases (down arrow) upon prolonged irradiation. Spectra were recorded at 1 min intervals during irradiation. (a) **11**. Note that the data are consistent with the presence of a band at ~290 nm whose intensity arguably increases in time. (b) **17**.

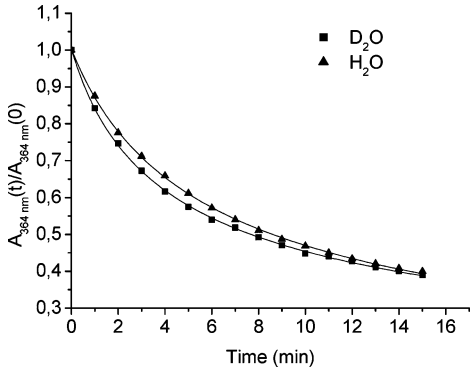

FIGURE 9. Photoinduced changes in aqueous solutions of compound **11** as monitored by recording the absorbance of the solution at 364 nm as a function of the elapsed photolysis time at 400 nm. The data indicate that the degradation reaction proceeds at a slightly faster rate in D_2O than in H_2O. An arbitrary fitting function has been applied to the data (i.e., neither first- nor second-order kinetics are observed).

faster in D_2O than in H_2O (Figure 9). Because the lifetime of singlet oxygen is longer in D_2O than it is in H_2O,[50,64]

(64) Ogilby, P. R.; Foote, C. S. *J. Am. Chem. Soc.* **1983**, *105*, 3423−3430.

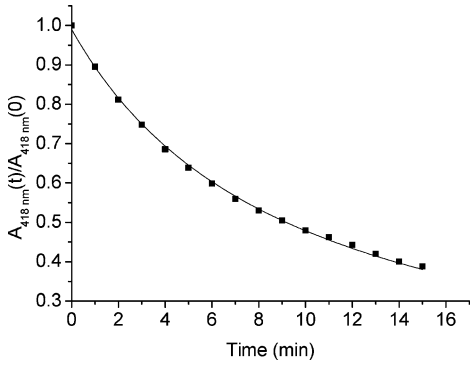

FIGURE 10. Photoinduced changes in an aqueous solution of compound **17** as monitored by recording the absorbance of the solution at 418 nm as a function of the elapsed photolysis time at 400 nm. A second-order decay function has been applied to the experimental data.

such data are generally interpreted to indicate that singlet oxygen is involved in the degradation process. In contrast, we did not observe a D_2O/H_2O solvent isotope effect on the rate of photoinduced change in a solution of **17**. Thus, it appears that, for these two compounds, different reactions may be involved in the degradation process. In support of this, we found that the decay of **11** did not follow either first- or second-order kinetics over the reaction period. On the other hand, the decay of **17** followed second-order kinetics over a comparatively long period of irradiation (Figure 10). These preliminary data indicate that a complete study of these degradation mechanism(s) exceeds the scope of the present report.

We conclude this discussion by noting that singlet oxygen quantum yields obtained using these molecules as sensitizers were recorded under conditions in which negligible bleaching had occurred. Nevertheless, in a series of experiments performed in toluene, we ascertained that the quantum yield of singlet oxygen production upon irradiation at 355 nm remains unchanged with the extent of degradation. In the least, these latter results should establish confidence in the data shown in Table 1.

E. Two-Photon Photosensitized Production of Singlet Oxygen. In our previous work,[22] we demonstrated that we could produce and optically detect singlet oxygen in a time-resolved experiment upon two-photon irradiation of 5,10,15,20-tetrakis(*N*-methyl-4-pyridyl)-21*H*,23*H*-porphine dissolved in water. In our present study, it remains for us to demonstrate that singlet oxygen can similarly be generated and detected using one of our phenylene−vinylene-based sensitizers. To this end, **17** was irradiated at 800 nm using the output of our femtosecond laser system. Experiments were performed in both D_2O and H_2O, using a dye concentration of 4×10^{-4} M. Under these conditions, we detected the 1270 nm phosphorescence of singlet oxygen in single photon counting experiments. As required for a process of two-photon excitation, the intensity of these singlet oxygen phosphorescence signals scales according to the square of the power of the irradiating laser (Figure 11). Thus, we can indeed produce singlet oxygen in water upon two-photon excitation of an OPV sensitizer with an electron donor−acceptor architecture.

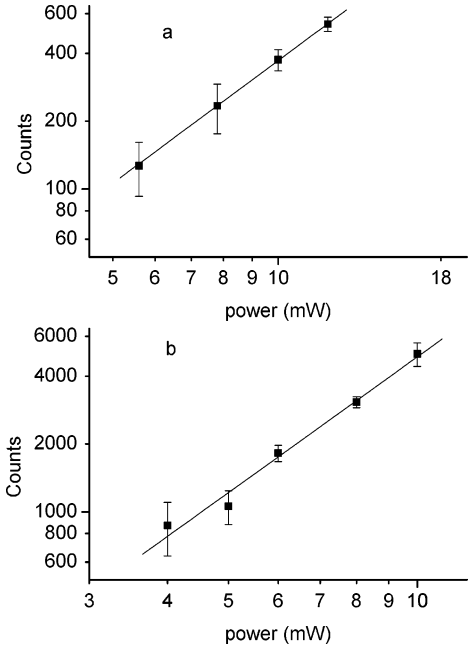

FIGURE 11. Double logarithmic plot of the singlet oxygen phosphorescence intensity against the average laser power incident on the sample. These data were recorded upon 800 nm irradiation of aqueous solutions of **17**. (a) Experiments performed in H_2O with 0.44 mM of **17**. A slope of 2.1 ± 0.4 was obtained. (b) Experiments performed in D_2O with 0.38 mM of **17**. A slope of 2.0 ± 0.2 was obtained.

The two-photon absorption profile of a compound also provides important information about the energies of accessible states. Using a technique described previously[22] in which we monitor the intensity of singlet oxygen phosphorescence produced as a function of the wavelength of light used to irradiate a given molecule, we can generate a two-photon action spectrum. When calibrated against the corresponding action spectrum obtained from a standard molecule, one can obtain the two-photon absorption spectrum. Such a spectrum is shown in Figure 12 for compound **17** dissolved in toluene. The reference standard used in this case was 2,5-dicyano-1,4-bis-(2-(4-diphenylaminophenyl)vinyl)benzene, CNPhVB.[22] Although values reported for the absolute TPA cross section of CNPhVB at its peak maximum cover a large range,[1,23,65] the data indicate that the molecule has a comparatively large TPA cross section (e.g., (1890 ± 280) × 10^{-50} cm^4 s $photon^{-1}$ $molecule^{-1}$ at ~840 nm). As such, the TPA cross section for **17** at 775 nm is appreciable.

Conclusion

In conclusion, we have shown that viable water-soluble two-photon singlet oxygen sensitizers can be constructed using an electron donor−acceptor OPV architecture. In two different approaches, water solubility was achieved through the use of specific substituents covalently attached to the sensitizer. In most cases examined, these substituents were an integral part of the chromophore. For OPV sensitizers in which solubility derived from the use of triethylene glycol substituents, singlet oxygen was produced with moderate efficiency. On the other hand, for sensitizers in which water solubility derived from ionic substituents (e.g., salts of *N*-methylpyridyl moieties), singlet oxygen was not produced in appreciable yield. These data provide insight into features of a given molecule important in the process of energy transfer to produce singlet oxygen. Of particular concern in this regard are the extent to which rapid charge transfer-mediated processes can deactivate sensitizer excited states at the exclusion of singlet oxygen production.

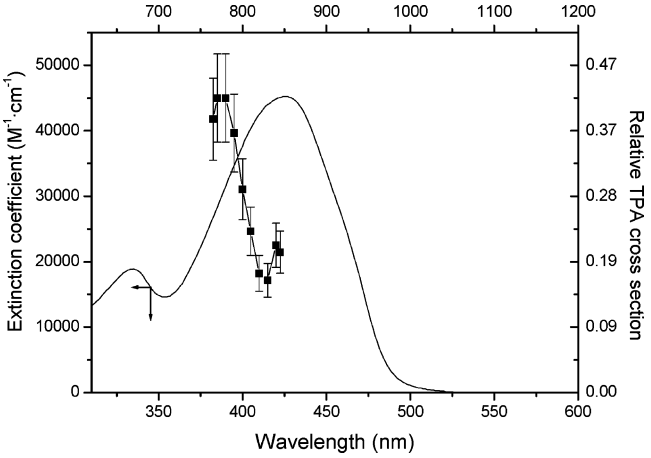

FIGURE 12. One-photon absorption spectrum (bottom and left-side axes) and two-photon action spectrum (top and right-side axes) for compound **17** in toluene. The two-photon spectrum was recorded by monitoring the intensity of singlet oxygen phosphorescence as a function of the wavelength of light used to irradiate **17**, calibrating each point against the corresponding signal from a reference standard.[22] The wavelength range accessible for the two-photon spectrum is limited by the range over which the femtosecond laser used can be tuned.

Experimental Section

Synthesis. The detailed procedures used to synthesize the compounds discussed in this work, along with the associated characterization data, are provided in the Supporting Information.

Photophysical Methods. All measurements were performed using spectroscopic grade solvents.

A. Sensitizer Fluorescence Experiments. Solutions were degassed for 15 min with argon prior to use. Data were recorded using an instrument composed of a 450 W Xe lamp for steady-state measurements and a diode laser for lifetime measurements. The detection system was a single photon-counting photomultiplier tube in a peltier-cooled housing. All spectra were measured in a perpendicular geometry using 1 cm quartz cuvettes. Steady-state measurements were obtained with 1.8 nm band-pass filters and corrected for wavelength-dependent intensity variation of the excitation light source. Quantum yields were determined using 9,10-diphenylanthracene in cyclohexane ($\phi_f = 0.93 \pm 0.03$)[66] as the fluorescence standard with refractive index and differential absorption corrections. In all cases, time-resolved fluorescence decay traces were single-exponential, and lifetimes were determined using least-squares analysis. All time-resolved measurements were conducted with 7.3 nm band-pass filters. Experiments were performed using dye concentrations of ~5 × 10^{-6} M where the sample absorbance was ~0.2−0.3.

(65) Zhang, B.-J.; Jeon, S.-J. *Chem. Phys. Lett.* **2003**, *377*, 210−216.

(66) Meech, S. R.; Phillips, D. *J. Photochem.* **1983**, *23*, 193−217.

B. Singlet Oxygen Experiments. Details of the instrumentation and approach used to produce and optically detect singlet oxygen in both one- and two-photon experiments are presented elsewhere.[19,22,67] For some of the one-photon experiments, the near-IR output of our femtosecond laser system was frequency-doubled in a β-barium borate crystal to yield a suitable UV−vis wavelength with which to irradiate the sensitizer (e.g., 800 nm → 400 nm; energy < 0.4 μJ/pulse). Otherwise, the sensitizer was irradiated with the output of a nanosecond Nd:YAG laser system (energy < 0.3 mJ/pulse). For data recorded in water (e.g., Figure 4a), the fitting function derived from eq 1 was extrapolated to time = 0 and then integrated to yield an intensity suitable for comparison to that obtained from the reference standard. For data recorded in toluene, where $k_T \gg k_{decay}$, eq 1 reduces to a single-exponential decaying function. In this case, both the signal intensity at time = 0 as well as the integral of the signal were used in the comparison to the reference standard.

C. Triplet State Absorption Measurements. Details of the instrumentation and approach used for the time-resolved absorption measurements are published elsewhere.[67]

D. Photoacoustic Experiments. Time-resolved photoacoustic signals were monitored after pulsed laser irradiation using a home-built piezoelectric transducer. The general approach used has been outlined previously.[59] Irradiation energies used were approximately 20 μJ/pulse. Data were analyzed using a commercially available deconvolution routine (Sound Analysis 1.50D, Quantum Northwest).

E. Two-Photon Experiments. Details of the instrumentation and approach used to quantify TPA cross sections and action spectra are published elsewhere.[22]

Acknowledgment. This work was funded by the Villum Kann Rasmussen Foundation and by the Danish Natural Science Research Council through a block grant for The Center for Oxygen Microscopy. We thank (1) Silvia Braslavsky (Max Planck Institute, Mülheim) for the photoacoustic transducer used in these experiments, (2) Frederik C. Krebs and Holger Spanggaard (Risø National Laboratories) for valuable discussions, and (3) Flemming Hansen for collecting the crystallographic data and the Center for Crystallographic Studies, University of Copenhagen, for the use of their equipment.

Supporting Information Available: Synthetic procedures and characterization of all compounds prepared. This material is available free of charge via the Internet at http://pubs.acs.org.

JO050507Y

(67) Keszthelyi, T.; Weldon, D.; Andersen, T. N.; Poulsen, T. D.; Mikkelsen, K. V.; Ogilby, P. R. *Photochem. Photobiol.* **1999**, *70*, 531−539.